Nonlinear Dyn (2014) 77:1157–1170
DOI 10.1007/s11071-014-1368-3

ORIGINAL PAPER

# Development of a family of explicit algorithms for structural dynamics with unconditional stability

**Yao Gui · Jin-Ting Wang · Feng Jin · Cheng Chen · Meng-Xia Zhou**

Received: 27 October 2013 / Accepted: 14 March 2014 / Published online: 2 April 2014


**Abstract** A new family of explicit integration algorithms is developed based on discrete control theory for solving the dynamic equations of motion. The proposed algorithms are explicit for both displacement and velocity and require no factorisation of the damping matrix and the stiffness matrix. Therefore, for a system with nonlinear damping and stiffness, the proposed algorithms are more efficient than the common explicit algorithms that provide only explicit displacement. Accuracy and stability properties of the proposed algorithms are analysed theoretically and verified numerically. Certain subfamilies are found to be unconditionally stable for any system state (linear elastic, stiffness softening or stiffness hardening) that may occur in earthquake engineering of a practical structure. With dual explicit expression and excellent stability property, the proposed family of algorithms can potentially solve complicated nonlinear dynamic problems.

**Keywords** Explicit algorithm · Nonlinear structural dynamics · Stability · Computational efficiency · Discrete transfer function

Y. Gui · J.-T. Wang · F. Jin (✉) · M.-X. Zhou
State Key Laboratory of Hydroscience and Engineering, Tsinghua University, Beijing 100084, China
e-mail: jinfeng@tsinghua.edu.cn

C. Chen
School of Engineering, San Francisco State University, San Francisco, CA 94132, USA

## 1 Introduction

Step-by-step time-integration algorithms are widely used to solve the equations of motion of structures. Generally, the integration algorithms can be classified into two types: explicit and implicit. An integration algorithm is defined as explicit if the displacements for the next step can be calculated based on the conditions known at the beginning of the time step, whereas an implicit integration algorithm exhibits dependency on the structural response from the next step.

Both the explicit and implicit algorithms have obvious advantages and disadvantages [1]. Most implicit integration algorithms are unconditionally stable, such as the average acceleration method [2], Wilson-$\theta$ method [3], HHT-$\alpha$ method [4] and WBZ-$\alpha$ method [5]. However, they have to solve the simultaneous equations resulting from discretisation of the equations of motion in spatial and temporal domains. The computational cost dramatically increases when the degrees-of- freedom (DOFs) of the structure get large. The explicit algorithms require no factorisation of the stiffness matrix and have clear advantages for problems with a large number of DOFs. Conditional stability is the drawback of the traditional explicit integration algorithms such as the central difference method (CDM) and the explicit Newmark method [2]. Their time step limit is inversely proportional to the highest natural frequency of structures. To improve the numerical properties of integration algorithms, researchers have pro-

posed subcycling strategies [6] and high-order accurate approaches [7].

Several unconditionally stable explicit integration algorithms have been proposed, including the Chang family of algorithms [8–10] and the CR algorithm [11]. The Chang family of algorithms has excellent stability, and one of its subfamilies offers unconditional stability even for stiffness hardening systems that may occur in practice. However, similar to the CDM and explicit Newmark method, the Chang family is explicit only if the damping matrix is diagonal. Therefore, for system equipped with nonlinear dampers [12,13], these explicit algorithms have no advantage of computational efficiency as compared to implicit algorithms. To explicitly solve the equation of motion for system with nonlinear damping, Chen and Ricles [11] use the pole mapping method to develop the CR algorithm, which provides an explicit estimate of velocity as well as displacement. This method is shown to be unconditionally stable for any linear elastic and stiffness softening system and is conditionally stable for a stiffness hardening system.

The accuracy and stability properties of integration algorithms are usually investigated in the time domain by using the amplification matrix and its associated eigenvalues [14–16]. Researchers have also analysed the frequency domain properties of integration algorithms by using the discrete transfer function and its associated poles. A discrete transfer function is used to represent the relationship between the $z$ transform of the output and the $z$ transform of the input [17]. Ramirez [18] derived the discrete transfer function for the Newmark family of algorithms and studied their frequency response characteristics. Magnitude and phase error characteristics of some popular algorithms are studied in the frequency domain by Mugan and Hulbert [19,20]. Chen and Ricles [21,22] used the root locus method to analyse the stability of integration algorithms under stiffness nonlinear structural behaviour.

In this paper, a new family of explicit integration algorithms with second-order accuracy, including the CR algorithm as a special case, is developed based on the pole mapping method from the discrete control theory. Both accuracy and stability properties are analytically studied and numerical examples are examined to confirm the theoretical analysis results. The proposed family of algorithms is found to have the same numerical properties as the Newmark family of algorithms for linear elastic systems. More significantly, certain subfamilies are unconditionally stable for any system state (linear elastic, stiffness softening, or stiffness hardening). As an example, comparison of the computational cost is presented for several integration algorithms in solving a system with nonlinear damping behaviour. The comparison demonstrates that the proposed family of algorithms offers distinct advantage in computational efficiency.

## 2 Development of the new family of algorithms

For a multiple-degree-of-freedom (MDOF) nonlinear structure, the equations of motion can be expressed as

$$\mathbf{M}\ddot{\mathbf{x}}_{i+1} + \mathbf{R}(\dot{\mathbf{x}}_{i+1}) + \mathbf{R}(\mathbf{x}_{i+1}) = \mathbf{F}_{i+1}, \tag{1}$$

where $\mathbf{M}$ is the mass matrix; $\mathbf{R}(\dot{\mathbf{x}}_{i+1})$, $\mathbf{R}(\mathbf{x}_{i+1})$ and $\mathbf{F}_{i+1}$ are the damping force, restoring force and external force vectors at the $(i+1)$ th time step, respectively, and $\mathbf{x}_{i+1}$, $\dot{\mathbf{x}}_{i+1}$ and $\ddot{\mathbf{x}}_{i+1}$ are the displacement, velocity and acceleration vectors at the $(i+1)$th time step, respectively.

A family of integration algorithms, where the velocity vector $\dot{\mathbf{x}}_{i+1}$ and displacement vector $\mathbf{x}_{i+1}$ are dependent only on structural response (displacement, velocity and acceleration) at the $i$th time step, are assumed as

$$\dot{\mathbf{x}}_{i+1} = \dot{\mathbf{x}}_i + \boldsymbol{\alpha}_1 \cdot \Delta t \cdot \ddot{\mathbf{x}}_i \tag{2}$$

$$\mathbf{x}_{i+1} = \mathbf{x}_i + \Delta t \cdot \dot{\mathbf{x}}_i + \boldsymbol{\alpha}_2 \cdot \Delta t^2 \cdot \ddot{\mathbf{x}}_i, \tag{3}$$

where $\boldsymbol{\alpha}_1$ and $\boldsymbol{\alpha}_2$ are two matrices of integration parameters to be determined; and $\Delta t$ is the time step size. Equation (1) can be explicitly integrated with Eqs. (2) and (3), when $\boldsymbol{\alpha}_1$ and $\boldsymbol{\alpha}_2$ are known.

For simplicity, parameters $\boldsymbol{\alpha}_1$ and $\boldsymbol{\alpha}_2$ are derived from a single-degree-of-freedom (SDOF) linear elastic structure in the following. Correspondingly, Eqs. (1), (2) and (3) are rewritten as

$$m\ddot{x}_{i+1} + c\dot{x}_{i+1} + kx_{i+1} = F_{i+1} \tag{4}$$

$$\dot{x}_{i+1} = \dot{x}_i + \alpha_1 \cdot \Delta t \cdot \ddot{x}_i \tag{5}$$

$$x_{i+1} = x_i + \Delta t \cdot \dot{x}_i + \alpha_2 \cdot \Delta t^2 \cdot \ddot{x}_i, \tag{6}$$

where $m$, $c$ and $k$ are the mass, viscous damping and stiffness, respectively; $F_{i+1}$ is the external force at the $(i+1)$th time step and $x_{i+1}$, $\dot{x}_{i+1}$ and $\ddot{x}_{i+1}$ are the displacement, velocity and acceleration at the $(i+1)$th time step, respectively.

Next, we will determine the parameters $\alpha_1$ and $\alpha_2$. The derivation of parameters $\alpha_1$ and $\alpha_2$ for SDOF linear elastic systems is provided in Sects. 2.1 and 2.2 based on the pole mapping method and the eigenvalue mapping method, respectively. Then the integration process of the proposed family of algorithms for nonlinear MDOF systems is briefly described in Sect. 2.3. The numerical properties of proposed algorithms for both linear and nonlinear systems are discussed in Sect. 3.

## 2.1 The pole mapping method

We define $X_i(z)$ and $X_{i+1}(z)$ as the $z$ transform of a time function $x(t)$ at the $i$th and $(i+1)$th time step, respectively. According to the shifting theorem for the $z$ transform [23], multiplication of $X_{i+1}(z)$ by $z^{-1}$ delays the time function $x(t)$ by the time step

$$X_i(z) = z^{-1} \cdot X_{i+1}(z), \tag{7}$$

where $z$ is the variable of the $z$ transform.

Thus, the $z$ transform of Eqs. (4), (5) and (6) may be expressed as

$$m\ddot{X}_{i+1}(z) + c\dot{X}_{i+1}(z) + kX_{i+1}(z) = F_{i+1}(z) \tag{8}$$

$$\dot{X}_{i+1}(z) = z^{-1} \cdot \dot{X}_{i+1}(z) + \alpha_1 \cdot \Delta t \cdot z^{-1} \cdot \ddot{X}_{i+1}(z) \tag{9}$$

$$X_{i+1}(z) = z^{-1} \cdot X_{i+1}(z) + \Delta t \cdot z^{-1} \cdot \dot{X}_{i+1}(z) + \alpha_2 \cdot \Delta t^2 \cdot z^{-1} \cdot \ddot{X}_{i+1}(z), \tag{10}$$

where $X_{i+1}(z)$, $\dot{X}_{i+1}(z)$, $\ddot{X}_{i+1}(z)$ and $F_{i+1}(z)$ are the $z$ transform of $x_{i+1}$, $\dot{x}_{i+1}$, $\ddot{x}_{i+1}$ and $F_{i+1}$, respectively.

Substituting Eqs. (9) and (10) into Eq. (8) leads to the corresponding discrete transfer function

$$G(z) = \frac{X_{i+1}(z)}{F_{i+1}(z)} = \frac{\alpha_2 \Delta t^2 z + (\alpha_1 - \alpha_2)\Delta t^2}{mz^2 + (\alpha_2 \Omega^2 + 2\alpha_1 \Omega\xi - 2)mz + ((\alpha_1 - \alpha_2)\Omega^2 - 2\alpha_1 \Omega\xi + 1)m}, \tag{11}$$

where $\Omega = \omega_n \Delta t$, $\omega_n = \sqrt{k/m}$ is the natural frequency and $\xi$ is the viscous damping ratio.

Based on Eq. (11), the characteristic equation of the discrete system is defined as

$$mz^2 + (\alpha_2 \Omega^2 + 2\alpha_1 \Omega\xi - 2)mz + ((\alpha_1 - \alpha_2)\Omega^2 - 2\alpha_1 \Omega\xi + 1)m = 0. \tag{12}$$

A value of $z$ that solves the characteristic equation is defined as a 'pole' of the discrete transfer function.

**Table 1** Poles of some members of the Newmark family algorithms

| Method | Poles |
|---|---|
| Average acceleration method ($\gamma$ =1/2, $\beta$ =1/4) | $z_{1,2} = \frac{4-\Omega^2 \pm 4\Omega\sqrt{\xi^2-1}}{4+\Omega^2+4\Omega\xi}$ |
| Linear acceleration method ($\gamma$ =1/2, $\beta$ =1/6) | $z_{1,2} = \frac{6-2\Omega^2 \pm \Omega\sqrt{3\Omega^2+36\xi^2-36}}{6+\Omega^2+6\Omega\xi}$ |
| Explicit Newmark method ($\gamma = 1/2, \beta = 0$) | $z_{1,2} = \frac{2-\Omega^2 \pm \Omega\sqrt{\Omega^2+4\xi^2-4}}{2+2\Omega\xi}$ |

Chen and Ricles [11] showed that the poles of the discrete transfer function are the same as the eigenvalues of the amplification matrix for the Newmark family of algorithms. Therefore, in developing a new integration algorithm, the numerical properties of the integration algorithm are ensured if proper poles are assigned to its discrete transfer function.

The poles of several well-known members of the Newmark family of algorithms with second-order accuracy are listed in Table 1, where $\gamma$ and $\beta$ are the integration parameters of the Newmark method. By assigning these poles to the characteristic equation in Eq. (12), we find that $\alpha_1$ and $\alpha_2$ always have the same expression. Thus, they can be unified as one parameter

$$\alpha_1 = \alpha_2 = \alpha = \frac{\lambda}{\lambda + \lambda\Omega\xi + \Omega^2}, \tag{13}$$

where $\lambda$ is the positive parameter governing the numerical properties. The subfamily with $\lambda$ is derived from the Newmark family with $\gamma = 1/2, \beta = 1/\lambda$. As a result, the corresponding algorithms of the two families have the same numerical properties.

Comparing Eq. (13) with the integral algorithm developed by Chen and Ricels [11], we found that the subfamily with $\lambda = 4$ was exactly the same as the CR algorithm. Therefore, the proposed algorithms contained the well-known CR algorithm as a special case.

### 2.2 The eigenvalue mapping method

Besides the pole mapping method, a new integration algorithm may also be developed based on the eigenvalues of the amplification matrix.

Equations (4), (5) and (6) may be written in a recursive matrix form as

$$\mathbf{X}_{i+1} = \mathbf{A} \cdot \mathbf{X}_i + \mathbf{B} \cdot F_i, \tag{14}$$

where $\mathbf{X}_i$ and $\mathbf{X}_{i+1}$ are state vector values at the $i$th and $(i+1)$th time step, respectively; $\mathbf{A}$ is the amplification matrix and $\mathbf{B}$ is related to the external force. $\mathbf{X}_i$, $\mathbf{X}_{i+1}$, $\mathbf{A}$ and $\mathbf{B}$ are defined as

$$\mathbf{X}_i = \begin{bmatrix} x_i \\ \dot{x}_i \end{bmatrix}, \quad \mathbf{X}_{i+1} = \begin{bmatrix} x_{i+1} \\ \dot{x}_{i+1} \end{bmatrix} \tag{15}$$

$$\mathbf{A} = \begin{bmatrix} 1-\alpha_2\omega_{\mathrm{n}}^2\Delta t^2 & \Delta t - 2\alpha_2\xi\omega_{\mathrm{n}}\Delta t^2 \\ -\alpha_1\omega_{\mathrm{n}}^2\Delta t & 1-2\alpha_1\xi\omega_{\mathrm{n}}\Delta t \end{bmatrix},$$

$$\mathbf{B} = \begin{bmatrix} \alpha_2\Delta t^2/m \\ \alpha_1\Delta t/m \end{bmatrix}. \tag{16}$$

The characteristic equation of the amplification matrix $\mathbf{A}$ can be derived by solving the equation of $|\mathbf{A} - \phi\mathbf{I}| = 0$ and is found to be

$$\phi^2 + (\alpha_2\Omega^2 + 2\alpha_1\Omega\xi - 2)\phi + (\alpha_1 - \alpha_2)\Omega^2 - 2\alpha_1\Omega\xi + 1 = 0, \tag{17}$$

where $\phi$ is the eigenvalue and $\mathbf{I}$ is a unit matrix.

Equation (17) is identical to the characteristic equation of the discrete transfer function Eq. (11). This verifies the conclusion made by Chen and Ricles [11] that the poles of the discrete transfer function are the same as the eigenvalues of the amplification matrix for the integration algorithm. Therefore, the eigenvalue mapping method is equivalent to the pole mapping method.

### 2.3 Integration process for nonlinear MDOF systems

For an MDOF system, Eq. (13) can be rewritten in terms of the structural properties and the time step size as

$$\boldsymbol{\alpha}_1 = \boldsymbol{\alpha}_2 = \boldsymbol{\alpha} = 2\lambda \cdot (2\lambda\mathbf{M} + \lambda\Delta t\mathbf{C} + 2\Delta t^2\mathbf{K})^{-1} \cdot \mathbf{M}. \tag{18}$$

If the MDOF system is nonlinear, $\boldsymbol{\alpha}$ is assumed to be invariant in the entire integration procedure and is determined from the initial damping matrix $\mathbf{C}_0$ and the initial stiffness matrix $\mathbf{K}_0$

$$\boldsymbol{\alpha} = 2\lambda \cdot (2\lambda\mathbf{M} + \lambda\Delta t\mathbf{C}_0 + 2\Delta t^2\mathbf{K}_0)^{-1} \cdot \mathbf{M}. \tag{19}$$

Thus, the solution of Eq. (1) using the proposed algorithms may be summarised as follows: (1) substituting Eq. (19) into Eqs. (2) and (3) leads to the velocity vector $\dot{\mathbf{x}}_{i+1}$ and displacement vector $\mathbf{x}_{i+1}$; (2) the nonlinear damping force $\mathbf{R}(\dot{\mathbf{x}}_{i+1})$ and restoring force $\mathbf{R}(\mathbf{x}_{i+1})$ are calculated and (3) the acceleration vector $\ddot{\mathbf{x}}_{i+1}$ is obtained from the equations of motion in Eq. (1).

## 3 Numerical properties

### 3.1 Accuracy analysis

Since the numerical properties of an integration algorithm are determined by the poles of the algorithm [11] and the proposed algorithm family has the same poles as those of the Newmark family of algorithms, the proposed family of algorithms is second-order accurate, which is the same as most commonly used algorithms. Herein, the amplitude decay (AD) and period elongation (PE) [24] are introduced to further analyse the computational error of these algorithms. Following Refs. [5,8,11,24,25], we consider the linear free vibration problem

$$m\ddot{x}(t) + kx(t) = 0 \tag{20}$$

with the initial conditions $x(0) = 1$ and $\dot{x}(0) = 0$. The AD and PE are defined as

$$\mathrm{AD} = 1 - x(\bar{T}_{\mathrm{n}}) \tag{21}$$

$$\mathrm{PE} = (\bar{T}_{\mathrm{n}} - T_{\mathrm{n}})/T_{\mathrm{n}}, \tag{22}$$

where $T_{\mathrm{n}}$ and $\bar{T}_{\mathrm{n}}$ represent the true and calculated natural period, respectively.

When the equation for an integration algorithm is known, the poles for its corresponding discrete transfer function $G(z)$ can be expressed in an exponential form as

$$z_{1,2} = \sigma \pm \varepsilon i = \exp\left[\bar{\Omega}\left(-\bar{\xi} \pm i\sqrt{1-\bar{\xi}^2}\right)\right], \tag{23}$$

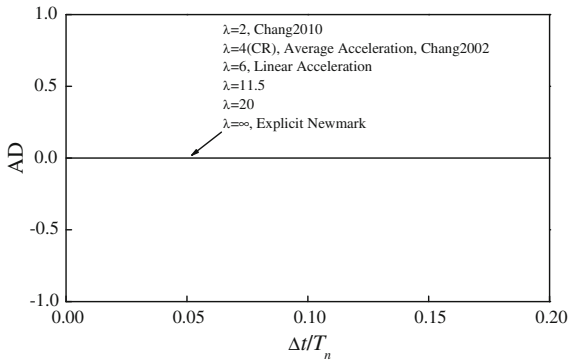


**Fig. 1** Amplitude decay for proposed family of algorithms, and comparison with Newmark and Chang families of algorithms

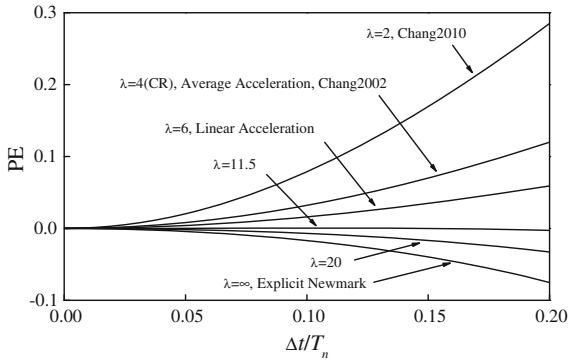


**Fig. 2** Period elongation for proposed family of algorithms, and comparison with Newmark and Chang families of algorithms

where $i = \sqrt{-1}$, and the algorithmic damping ratio $\bar{\xi}$ and the apparent frequency $\bar{\Omega}$ may be computed by

$$\bar{\xi} = -\ln(\sigma^2 + \varepsilon^2)/(2\bar{\Omega}) \tag{24}$$

$$\bar{\Omega} = \tan^{-1}(\varepsilon/\sigma)\Big/\sqrt{1-\bar{\xi}^2}. \tag{25}$$

Because of the zero inherent damping of the system, the AD completely depends on the algorithmic damping ratio $\bar{\xi}$. Meanwhile, substituting $\bar{T}_\mathrm{n} = 2\pi\Delta t/\bar{\Omega}$ into Eq. (22) results in

$$\mathrm{PE} = \Omega/\bar{\Omega} - 1. \tag{26}$$

Figures 1 and 2 show the variation of AD and PE with $\Delta t/T_\mathrm{n}$, respectively, for several members of the proposed family of algorithms, as well as the Newmark and Chang families of algorithms. The algorithms that have the same poles exhibit exactly the same AD and PE. As shown in Fig. 1, all of these algorithms predict no decay of displacement amplitude because

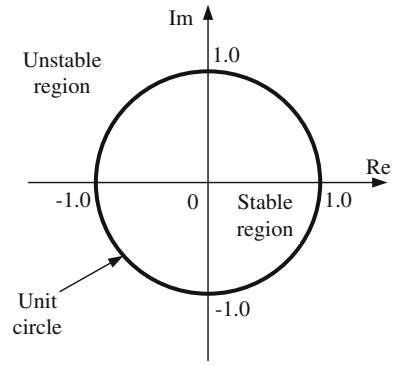


**Fig. 3** Stable and unstable regions for pole locations in the $z$ plane

their algorithmic damping ratios $\bar{\xi} = 0$. Figure 2 indicates that the absolute value of PE increases as $\Delta t/T_\mathrm{n}$ increases for a given $\lambda$. Meanwhile, the PE decreases as $\lambda$ increases from 0 to infinity for a given $\Delta t/T_\mathrm{n}$. The period distortion of the subfamily with $\lambda = 11.5$ is approximately the least for any $\Delta t/T_\mathrm{n}$. As a result, $\lambda$ should be chosen as close to 11.5 as possible to obtain the least period error.

## 3.2 Stability

According to the discrete control theory [23], the stability of a discrete transfer function is determined by the poles. Figure 3 illustrates the stable and unstable regions for pole locations in the $z$ plane. If all the poles lie within or on the unit circle, the system is stable. Any pole outside the unit circle makes the system unstable. Therefore, the stability condition of the proposed family of algorithms is determined in this section by analysing the poles of their discrete transfer functions. The linear and nonlinear systems are considered.

### *3.2.1 Linear elastic system*

For a linear elastic system, the discrete transfer function $G(z)$ and its characteristic equation are presented in Eqs. (11) and (12), respectively, for the proposed family of algorithms. The characteristic equation in Eq. (12) can be revised as

$$f(z) = A_1 z^2 + A_2 z + A_3 = 0, \tag{27}$$

where $A_1 = \Omega^2 + \lambda + \lambda\Omega\xi$, $A_2 = \lambda\Omega^2 - 2\Omega^2 - 2\lambda$ and $A_3 = \Omega^2 + \lambda - \lambda\Omega\xi$.

According to Eq. (27), the poles of $G(z)$ can be expressed as

$$z_{1,2} = \frac{-A_2 \pm \sqrt{(A_2)^2 - 4A_1A_3}}{2A_1} \tag{28}$$

(1) If $(A_2)^2 - 4A_1A_3 < 0$ in Eq. (28), $z_{1,2}$ is complex numbers. The modulus of $z_{1,2}$ is

$$|z_{1,2}| = \sqrt{\left(-\frac{A_2}{2A_1}\right)^2 + \left(\frac{\sqrt{4A_1A_3 - (A_2)^2}}{2A_1}\right)^2} = \sqrt{\frac{A_3}{A_1}}. \tag{29}$$

In this case, both $A_1$ and $A_3$ are positive, and $A_3$ is not more than $A_1$. This observation means that the stability condition of $|z_{1,2}| \leq 1$ is always satisfied if $(A_2)^2 - 4A_1A_3 < 0$. Thus, the stability condition can be derived from $(A_2)^2 - 4A_1A_3 < 0$ as

$$\lambda\Omega^2 - 4\Omega^2 - 4\lambda < -4\lambda\xi^2 \tag{30}$$

(2) If $(A_2)^2 - 4A_1A_3 \geq 0$, then $z_{1,2}$ is real numbers. Because Eq. (27) represents a parabolic curve opening upward, the stability condition of $|z_{1,2}| \leq 1$ leads to the following inequalities:

$$f(1) \geq 0, \quad f(-1) \geq 0, \quad -1 \leq -\tfrac{A_2}{2A_1} \leq 1. \tag{31}$$

From the inequalities in Eq. (31) and $(A_2)^2 - 4A_1A_3 \geq 0$, the stability condition can be derived as

$$-4\lambda\xi^2 \leq \lambda\Omega^2 - 4\Omega^2 - 4\lambda \leq 0. \tag{32}$$

Combining Eqs. (30) and (32) leads to the following stability condition of the proposed family of algorithms for the linear elastic system:

$$(\lambda - 4)\Omega^2 - 4\lambda \leq 0. \tag{33}$$

Equation (33) provides the stability limit of $\Omega$ for the proposed family of algorithms

(1) If $\lambda \leq 4$, $\Omega \leq \infty$;
(2) If $\lambda > 4$, $\Omega \leq \sqrt{4\lambda/(\lambda - 4)}$.

Therefore, the subfamilies with $\lambda \leq 4$ are unconditionally stable for any linear elastic structure; the subfamilies with $\lambda > 4$ can become unstable when $\Omega > \sqrt{4\lambda/(\lambda - 4)}$. These results verify that the subfamily with $\lambda$ has the same stability condition as the Newmark family with $\gamma = 1/2$, $\beta = 1/\lambda$ for the linear elastic system [24].

### 3.2.2 System with nonlinear stiffness

For an SDOF structure with nonlinear stiffness, the equations of motion in Eq. (4) have to be expressed as

$$m\ddot{x}_{i+1} + c\dot{x}_{i+1} + r(x_{i+1}) = F_{i+1}, \tag{34}$$

where $r(x_{i+1})$ is the restoring force at the $(i+1)$th time step.

For a small time step size, Eq. (34) can be approximated in an incremental form

$$m\Delta\ddot{x}_i + c\Delta\dot{x}_i + k_t\Delta x_i = \Delta F_i, \tag{35}$$

where $k_t$ is the tangent stiffness for the $i$th time step; $\Delta\ddot{x}_i$, $\Delta\dot{x}_i$, $\Delta x_i$ and $\Delta F_i$ are the increments of acceleration, velocity, displacement and external force defined as $\Delta\ddot{x}_i = \ddot{x}_{i+1} - \ddot{x}_i$, $\Delta\dot{x}_i = \dot{x}_{i+1} - \dot{x}_i$, $\Delta x_i = x_{i+1} - x_i$ and $\Delta F_i = F_{i+1} - F_i$.

In Eq. (35), the tangent stiffness $k_t$ varies with the displacement $x_{i+1}$. Therefore, Eq. (35) corresponds to a closed-loop system [21]. The discrete transform function may be expressed in a closed-loop form as

$$G_{\mathrm{cl}}(z) = \frac{G'(z)}{1 + G'(z)H(z)}, \tag{36}$$

where $H(z)$ is the feedback transfer function, and $G'(z)H(z)$ is the open-loop transfer function of the closed-loop system.

When the proposed family of algorithms is used to solve Eq. (35), the corresponding closed-loop transfer function $G_{\mathrm{cl}}(z)$ relating $\Delta F_i$ and $\Delta x_i$ can be illustrated by the closed-loop block diagram shown in Fig. 4. The feedback transfer function $H(z)$ and the transfer function $G'(z)$ of $G_{\mathrm{cl}}(z)$ can be derived as

$$H(z) = k_t \tag{37}$$

$$G'(z) = \frac{\alpha\Delta t^2 z}{mz^2 + (\alpha c\Delta t - 2m)z + m - \alpha c\Delta t}. \tag{38}$$

Based on Eqs. (37) and (38), the characteristic equation of the closed-loop system in Eq. (35) is

$$1 + k_t\frac{\alpha\Delta t^2 z}{mz^2 + (\alpha c\Delta t - 2m)z + m - \alpha c\Delta t} = 0. \tag{39}$$

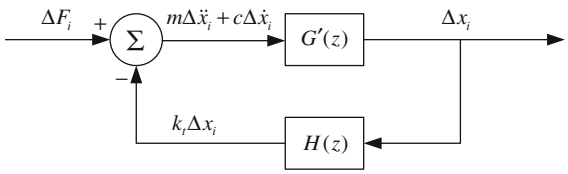


**Fig. 4** Closed-loop block diagram for system with nonlinear stiffness

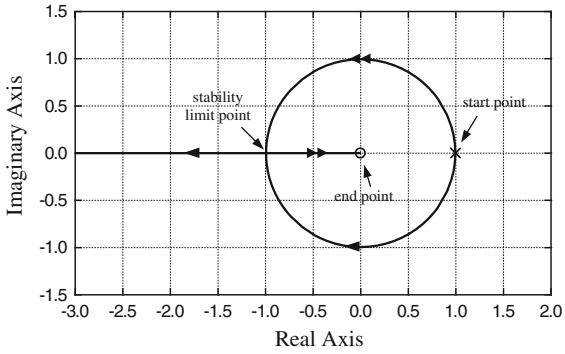


**Fig. 5** Root locus for system with nonlinear stiffness

For the linear elastic system, the tangent stiffness $k_t$ is equal to the initial stiffness $k_0$, and Eq. (39) reduces to the characteristic equation in Eq. (12).

The root locus method [17] is used to investigate the stability condition for the closed-loop system. This method involves plotting the root trajectories of the characteristic equation in the $z$ plane as the feedback gain parameter $k_t$ varies from zero to positive infinity. In this study, MATLAB [26] is used to plot the root locus.

The root locus for the case of $\xi = 0.02, \omega_n = 2\pi$ rad/s, $\Delta t = 0.5$s and $\lambda = 1$ is shown in Fig. 5. One branch of the locus crosses the unit circle at $z = -1$, which means that the proposed algorithms are stable only for a finite range of $k_t$. By substituting $z = -1$ into Eq. (39), the stability condition can be obtained as

$$k_t \alpha \Delta t^2 \leq 4m - 2\alpha c \Delta t \tag{40}$$

which can be rewritten as

$$\lambda(\Omega_t^2 - 4) \leq 4\Omega_0^2, \tag{41}$$

where $\Omega_0 = \omega_0 \Delta t$, and $\omega_0 = \sqrt{k_0/m}$ is the initial natural frequency; $\Omega_t = \omega_t \Delta t$, and $\omega_t = \sqrt{k_t/m}$ is the instantaneous natural frequency for the $i$th time step.

The stability condition in Eq. (41) reduces to that in Eq. (33) for a linear elastic system when $\Omega_t = \Omega_0$.

Equation (41) gives the stability range of $\lambda$

(1) If $\Omega_t \leq 2, \lambda \leq \infty$;
(2) If $\Omega_t > 2, \lambda \leq 4\Omega_0^2/(\Omega_t^2 - 4)$.

Thus, for stiffness softening systems, the subfamilies with $\lambda \leq 4$ are unconditionally stable; for stiffness hardening system, the unconditional stability range of $\lambda$ reduces to $\lambda \leq 4\omega_0^2/\omega_t^2$.

### 3.3 Discussion of numerical properties

Sections 3.1 and 3.2 indicate that the accuracy of the proposed family of algorithms improves as $\lambda$ increases from 0 to 11.5, the stability condition of $\Omega$ decreases as $\lambda$ increases from 4 to infinity for the linear elastic system and the stability condition of $\Omega_t$ decreases as $\lambda$ increases from $4\omega_0^2/\omega_t^2$ to infinity for the system with nonlinear stiffness. Therefore, the accuracy and stability are contradictory properties of the proposed family of algorithms.

Based on the theoretical analysis results, the subfamily with $\lambda = 4$ offers the highest accuracy within the unconditional stability range ($\lambda \leq 4$) for the linear elastic and stiffness softening systems. The subfamily with $\lambda = 4\omega_0^2/\omega_t^2$ (for instance, $\lambda = 2.77$, when $\omega_t = 1.2\omega_0$) offers the highest accuracy within the unconditional stability range ($\lambda \leq 4\omega_0^2/\omega_t^2$) for the stiffness hardening system.

## 4 Numerical examples

### 4.1 Dynamic response for MDOF linear elastic structure

An example is intentionally designed to confirm the stability limit and accuracy of the proposed family of algorithms for the linear system. As shown in Fig. 6, a two-storey shear-beam-type structure with $c_1 = c_2 = 0, k_1 = 2 \times 10^6$ N/m, $k_2 = 10^5$ N/m, $m_1 = 10^3$ kg, $m_2 = 4 \times 10^3$ kg is considered in this example. The structure is excited by a ground acceleration of $20\sin(t)$ at its base, and the time step $\Delta t = 0.05$s. The natural frequencies of the structure are 4.88 and 45.84 rad/s; thus, the values of $\Omega^{(1)}$ ($\Omega$ for the first mode) and $\Omega^{(2)}$ ($\Omega$ for the second mode) are 0.24 and

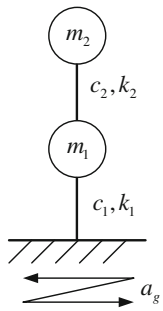


**Fig. 6** Schematic of the two-storey shear-beam-type structure

2.29, respectively. Applying Eq. (33) leads to the upper stability limit $\lambda_{\text{lim}}^{(2)} = 16.77$.

The displacement response of the top storey is plotted in Fig. 7 for $\lambda = 2, 4, 11.5, 17$ and $\infty$, respectively. And the result obtained from the explicit Newmark method ($\Delta t = 0.05$s and 0.0001s) and average acceleration method ($\Delta t = 0.05$s) are also shown in the same figure for comparison. Among them, the result from the explicit Newmark method with a time step of $\Delta t = 0.0001$s is seen as the 'exact' solution. As expected, the displacement responses of the subfamily with $\lambda = 4$ and the average acceleration method match each other very well; meanwhile, the subfamily with $\lambda = \infty$ and the explicit Newmark method get identical results. These solutions verify the conclusion in Sect. 3 that the subfamily of the proposed algorithm family has the same numerical properties as its corresponding subfamily in the Newmark family of algorithms for linear elastic systems. Because of the stability limit $\lambda \leq 16.77$, the solutions are unstable for the subfamilies with $\lambda = 17$ and $\infty$, whereas the subfamilies with $\lambda = 2, 4$ and 11.5 obtain reliable solutions. In addition, the subfamily with $\lambda = 11.5$ provides almost the same solution as the exact solution, whereas the subfamilies with $\lambda$ =2 and 4 exhibit obvious period elongation in the condition of $\Delta t / T_{\text{n}}^{(1)} = 0.039$. This observation is in good agreement with the accuracy analysis results presented in Fig. 2, where the subfamily with $\lambda = 11.5$ possesses the least period distortion for any value of $\Delta t / T_{\text{n}}$.

### 4.2 Dynamic response for MDOF structures with nonlinear stiffness

The numerical examples in Ref. [10] are employed in this study to confirm the stability property of the proposed family of algorithms for systems with nonlinear stiffness. In this example, a two-storey shear-beam-type structure, as shown in Fig. 6, with $c_1 = c_2 = 0$, $k_1 = 10^7$ N/m, $k_2 = 10^5$ N/m, $m_1 = 10^3$ kg, $m_2 = 6 \times 10^3$ kg is considered. The tangent stiffness for each storey is assumed to be in the form of

$$k_t = k_0[1 + 1.5\theta\sqrt{|\Delta u|}], \tag{42}$$

where $\Delta u$ is the interstorey displacement, and $\theta$ is the coefficient for simulating the two systems with different stiffness types. For the softening system, the coefficients of the bottom and top storeys are $\theta_1 = -0.1, \theta_2 = -0.2$, and for the hardening system, $\theta_1 = 1, \theta_2 = 2$. The structure is excited by a ground acceleration of $20\sin(t)$ at its base, and the time step $\Delta t = 0.05$s. The initial natural frequencies of the structure are 4.06 and 100.50 rad/s. For each system, the numerical result obtained from the explicit Newmark method with $\Delta t = 0.0001$s is considered as the 'exact' solution.

Figure 8 displays the displacement responses of the softening system for $\lambda = 2, 4, 4.7, 4.8$ and 11.5, respectively. The response time histories of instantaneous natural frequency for both modes are plotted in Fig. 9. The upper stability limit for the second mode

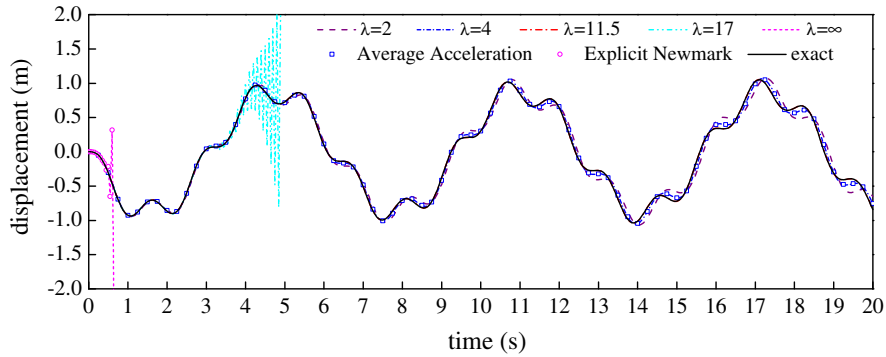


**Fig. 7** Displacement response of the top storey

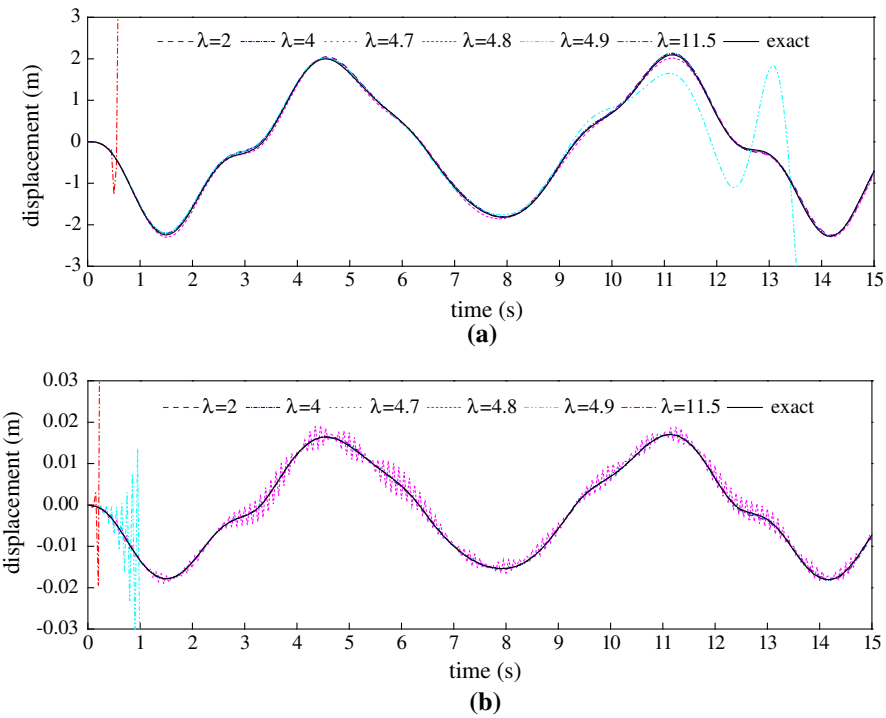


**Fig. 8** Displacement response of the stiffness softening system. **a** Displacement response of the top storey. **b** Displacement response of the bottom storey

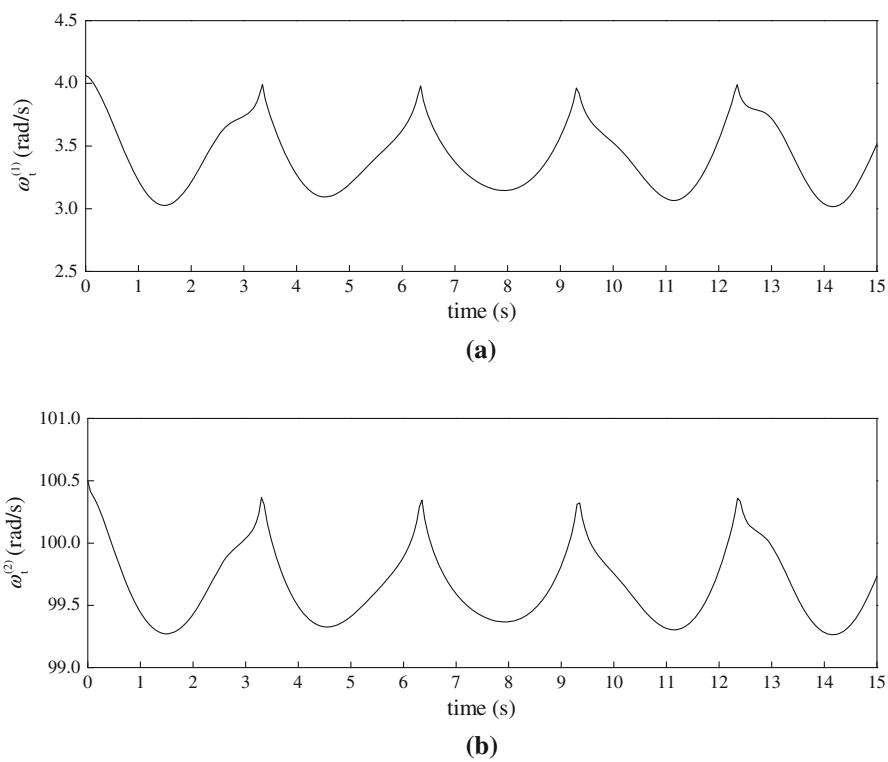


**Fig. 9** Instantaneous natural frequencies of the stiffness softening system. **a** Instantaneous natural frequency for first mode. **b** Instantaneous natural frequency for second mode

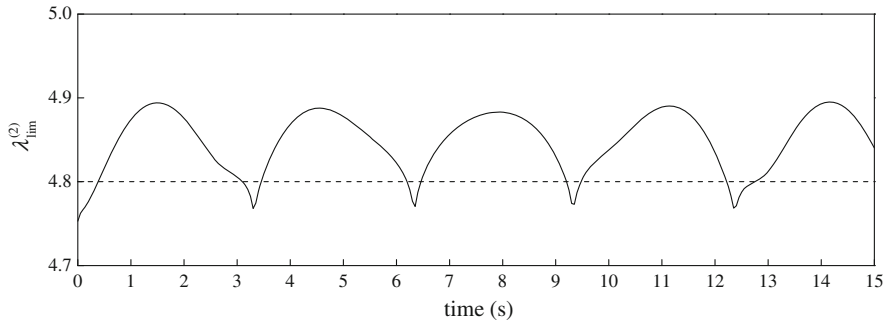


**Fig. 10** Upper stability limit for second mode of the stiffness softening system

is plotted in Fig. 10 (the stability condition $\Omega_t \leq 2$ is always satisfied for the first mode). Figure 8 reveals that the subfamilies with $\lambda = 2$ and 4 behave in a stable state for the value of $\Omega_0^{(2)}$ as large as 5.02. This finding is due to their unconditional stability for the softening system in which the instantaneous natural frequencies never exceed the initial natural frequencies as shown in Fig. 9. Besides, the response of the subfamily with $\lambda = 4.7$ is accurate, while numerical instability occurs for the subfamilies with $\lambda = 4.9$ and 11.5 because the least value of the upper stability limit is 4.75, as shown in Fig. 10. The bottom storey response of the subfamily with $\lambda = 4.8$ indicates high frequency fluctuation. The reason is that the upper stability limit is only transitorily violated, whereas the stability condition is satisfied most of the time as the stiffness softens, as shown in Figs. 9b and 10.

The numerical solutions of the hardening system for $\lambda = 1.2$, 3.7, 3.9, 4 and 11.5 are shown in Fig. 11. The response time histories of instantaneous natural frequency for both modes are presented in Fig. 12. The upper stability limit for the second mode is plotted in Fig. 13 (the stability condition $\Omega_t \leq 2$ is always satisfied for the first mode). Figure 11 indicates that the subfamily with $\lambda = 4$ becomes conditionally stable as

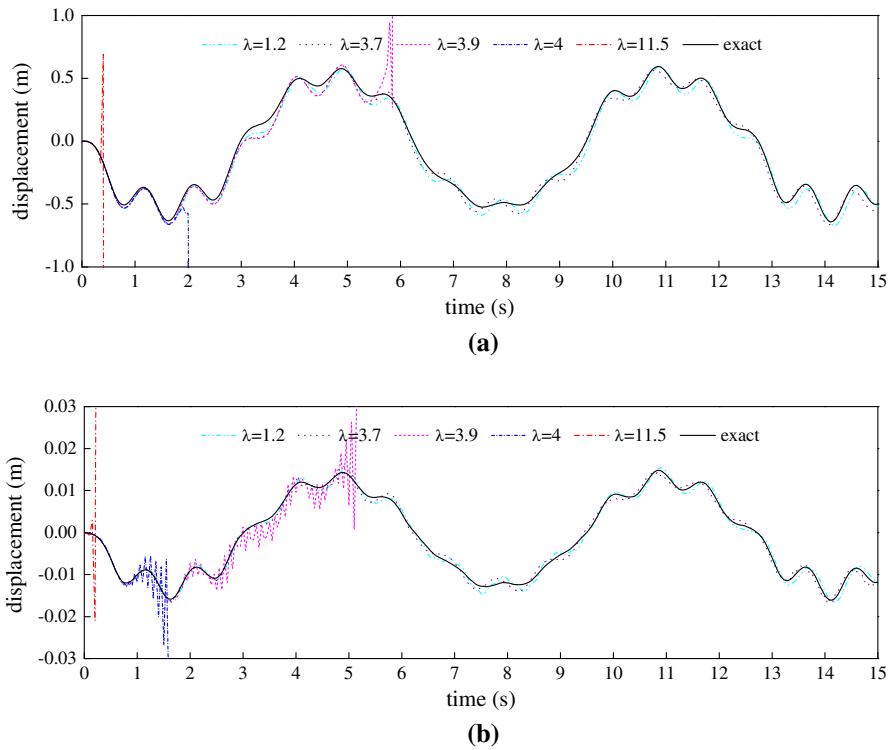


**Fig. 11** Displacement response of the stiffness hardening system. **a** Displacement response of the top storey. **b** Displacement response of the bottom storey

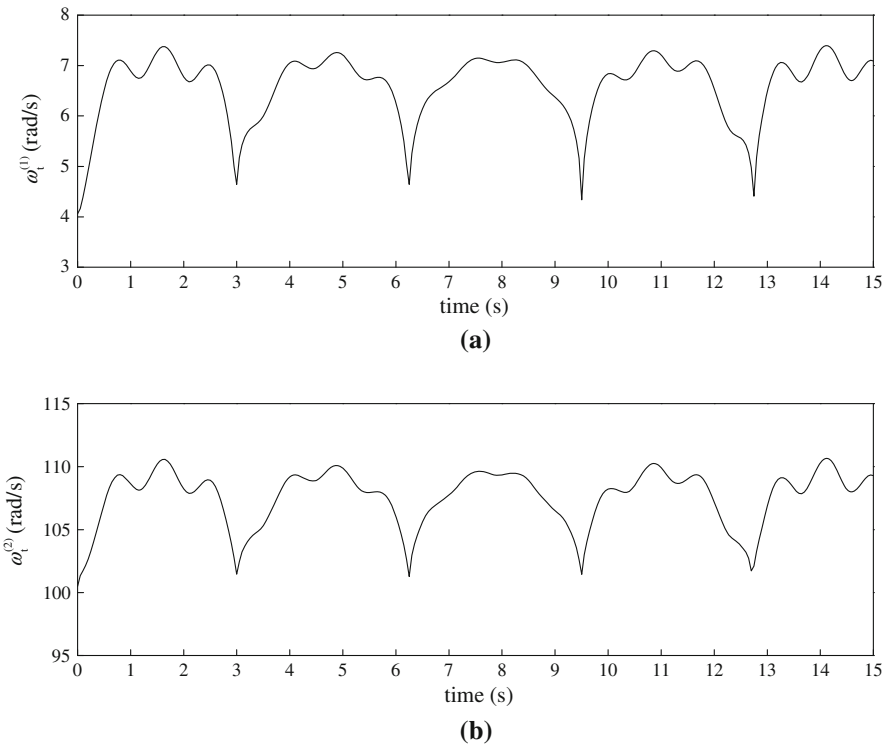


**Fig. 12** Instantaneous natural frequencies of the stiffness hardening system. **a** Instantaneous natural frequency for first mode. **b** Instantaneous natural frequency for second mode

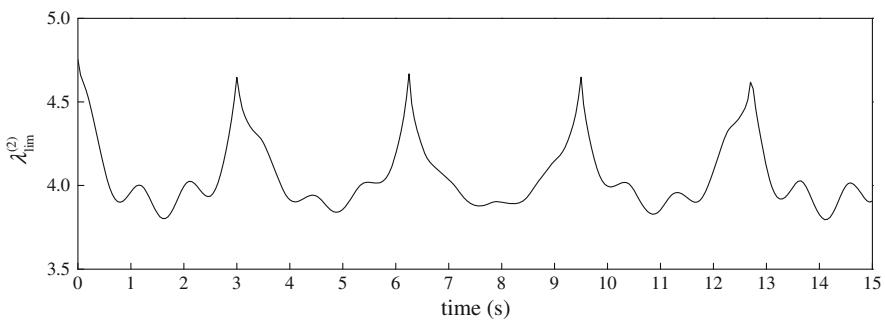


**Fig. 13** Upper stability limit for second mode of the stiffness hardening system

$\omega_t > \omega_0$ shown in Fig. 12. Meanwhile, the subfamily with $\lambda = 1.2 < 4(\omega_0^{(1)}/\omega_t^{(1)})^2$, which is unconditionally stable for this system, offers an acceptable solution. Figures 12b and 13 reveal that the upper stability limit decreases as the instantaneous natural frequency increases, and the least upper stability limit is 3.79 during the entire time history. As a result, stable computations are responsible for the subfamilies with $\lambda$ =1.2 and 3.7, whereas numerical instability occurs for the subfamilies with $\lambda = 3.9, 4$ and 11.5.

### 4.3 Computational times for MDOF structures with nonlinear damping

As shown in Fig. 14, an MDOF linear mass ($m_i$)–spring ($k_i$)–damping ($c_i$) system with nonlinear absolute damper ($c_{ai}$) is employed to compare the computational efficiency of three well-known algorithms and three proposed subfamilies. The parameters $m_i = 150$ kg, $k_i = 2.5 \times 10^5$ N/m, $c_i = 10$ Ns/m and $\Delta t = 0.02$ s are selected in these examples. Meanwhile, the absolute damping is provided by the magnetorheologi-

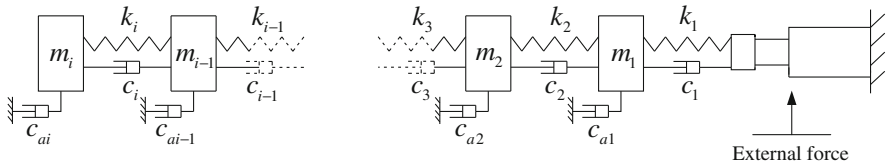


**Fig. 14** Schematic of the mass–spring–damping system with nonlinear damper

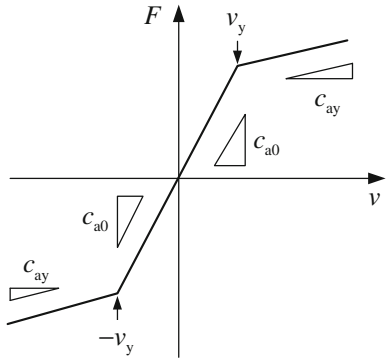


**Fig. 15** Force–velocity behaviour of the nonlinear biviscous model

cal damper (MRD). The nonlinear biviscous model [27] with $c_{a0} = 180$ Ns/m, $c_{ay} = 90$ Ns/m and $v_y = 1/3$ m/s is used to describe the force–velocity behaviour of the MRD, as shown in Fig. 15. The external input is a sine wave of 0.1-m amplitude and 1-Hz frequency.

The calculation procedures for all six algorithms with the number of DOFs ranging from 500 to 5,000 are implemented by a PC with Intel Core i7 3.4 GHz CPU and 8 GB internal memory. The average computational times for each task, which are measured by MATLAB [26], are presented in Table 2 and Fig. 16. The computational times for the average acceleration method, Chang2002 algorithm, and explicit Newmark method are broadly similar; they increase dramatically as the number of DOFs increases. Meanwhile, the relationships between the computational times for the subfamilies with $\lambda = 2, 4$ and 11.5 and the number of DOFs are all approximately linear. The computational time ratios of the first three algorithms to the proposed subfamilies grow significantly as the number of DOFs increases. The probable reason is that the explicit Newmark method and Chang2002 algorithm can provide only an explicit displacement and require factorising the damping matrix, and they both transform into 'implicit algorithms' when the damping matrix is non-diagonal, whereas the subfamilies being explicit for both displacement and velocity remain 'explicit algorithms'.

## 5 Conclusions

A discrete transfer function approach is used to develop a novel family of explicit algorithms for structural dynamics. This family of algorithms is based on expressions for displacement and velocity that are both explicit. The stability limit of the proposed family of algorithms is investigated based on control theory. The stability and accuracy characteristics of various subfamilies are confirmed by numerical examples for both linear elastic and stiffness nonlinear systems. The com-

**Table 2** Comparison of the computational times for various structure sizes

| DOFs | Computational times of each time step (ms) | | | | | |
|---|---|---|---|---|---|---|
| | Average acceleration | Chang2002 | Explicit Newmark | $\lambda = 2$ | $\lambda = 4$ | $\lambda = 11.5$ |
| 500 | 5.6 | 7.2 | 6.5 | 0.7 | 0.9 | 0.9 |
| 1,000 | 30.1 | 36.8 | 34.6 | 4.3 | 3.9 | 3.5 |
| 1,500 | 85.8 | 100.0 | 95.4 | 8.2 | 7.5 | 6.9 |
| 2,000 | 177.4 | 201.9 | 195.6 | 12.6 | 12.0 | 11.4 |
| 2,500 | 310.1 | 346.4 | 338.6 | 18.2 | 17.5 | 17.0 |
| 3,000 | 498.3 | 553.5 | 538.3 | 25.3 | 24.4 | 23.9 |
| 4,000 | 1,058.0 | 1,149.6 | 1,128.7 | 43.4 | 42.4 | 41.9 |
| 5,000 | 1,871.2 | 2,018.8 | 1,992.0 | 65.5 | 64.8 | 64.3 |

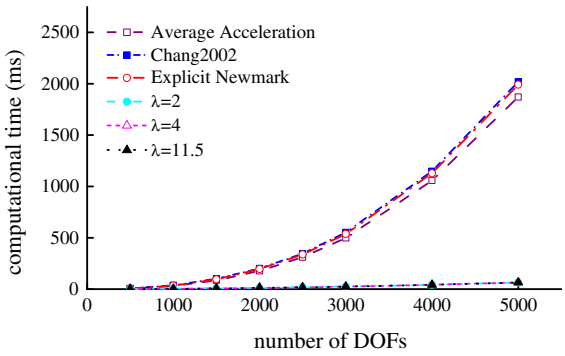


**Fig. 16** Graphical view of computational times for various structure sizes

putational efficiency of the new family for solving the system with nonlinear damping is compared with that of some well-known algorithms. The following conclusions are drawn:

(1) The proposed algorithm family requires no factorisation of the damping matrix and remains 'explicit algorithms' even though the damping matrix is non-diagonal; thus, it offers the obvious advantage of speed for the system with nonlinear damping.
(2) Each subfamily of the proposed algorithm family has the same numerical properties as its corresponding subfamily in the Newmark family of algorithms for linear elastic systems because they have the same poles for linear elastic systems.
(3) For the proposed family of algorithms, the period elongation decreases as $\lambda$ increases from 0 to infinity for a given $\Delta t/T_{\mathrm{n}}$. The period error of the subfamily with $\lambda = 11.5$ is approximately the least for any $\Delta t/T_{\mathrm{n}}$.
(4) The stability property decreases as $\lambda$ increases from 0 to infinity. The subfamilies with $\lambda \leq 4$ are unconditionally stable for any linear elastic system or stiffness softening system, whereas the subfamilies with $\lambda \leq 4\omega_0^2/\omega_t^2$ are unconditionally stable even for the stiffness hardening system.
(5) The accuracy and stability of the proposed family of algorithms are contradictory properties. To ensure unconditional stability and relatively high accuracy, the subfamily with $\lambda = 4$ (CR algorithm) is recommended for the linear elastic and stiffness softening systems, and the subfamily with $\lambda = 4\omega_0^2/\omega_t^2$ is recommended for the stiffness hardening system.

**Acknowledgments** This research is financially supported by the National Natural Science Foundation of China (Nos. 51179093, 91215301 and 41274106) and the Specialized Research Fund for the Doctoral Program of Higher Education (No. 20130002110032). The authors express their sincerest gratitude for these supports.

## References

1. Hussein, B., Negrut, D., Shabana, A.A.: Implicit and explicit integration in the solution of the absolute nodal coordinate differential/algebraic equations. Nonlinear Dyn. **54**(4), 283–296 (2008)
2. Newmark, N.M.: A method of computation for structural dynamics. J. Eng. Mech. Div. ASCE **85**(3), 67–94 (1959)
3. Wilson, E.L.: A computer program for the dynamic stress analysis of underground structures. Report UC SESM 68–1. University California, Berkeley (1968)
4. Hilber, H.M., Hughes, T.J., Taylor, R.L.: Improved numerical dissipation for time integration algorithms in structural dynamics. Earthq. Eng. Struct. D **5**(3), 283–292 (1977)
5. Wood, W., Bossak, M., Zienkiewicz, O.: An alpha modification of Newmark's method. Int. J. Numer. Methods Eng. **15**(10), 1562–1566 (1980)
6. Smolinski, P.: Subcycling integration with non-integer time steps for structural dynamics problems. Comput. Struct. **59**(2), 273–281 (1996)
7. Fung, T.: Higher-order accurate time-step-integration algorithms by post-integration techniques. Int. J. Numer. Methods Eng. **53**(5), 1175–1193 (2002)
8. Chang, S.Y.: Explicit pseudodynamic algorithm with unconditional stability. J. Eng. Mech. ASCE **128**, 935 (2002)
9. Chang, S.Y.: An explicit method with improved stability property. Int. J. Numer. Methods Eng. **77**(8), 1100–1120 (2009)
10. Chang, S.Y., Yang, Y.S., Hsu, C.W.: A family of explicit algorithms for general pseudodynamic testing. Earthq. Eng. Eng. Vib. **10**(1), 51–64 (2011)
11. Chen, C., Ricles, J.M.: Development of direct integration algorithms for structural dynamics using discrete control theory. J. Eng. Mech. ASCE **134**, 676 (2008)
12. Dong, X.M., Yu, M., Liao, C.R., Chen, W.M.: Comparative research on semi-active control strategies for magneto-rheological suspension. Nonlinear Dyn. **59**(3), 433–453 (2010)
13. Guo, P., Lang, Z., Peng, Z.: Analysis and design of the force and displacement transmissibility of nonlinear viscous damper based vibration isolation systems. Nonlinear Dyn. **67**(4), 2671–2687 (2012)
14. Hughes, T.J.: The Finite Element Method: Linear Static and Dynamic Finite Element Analysis. Prentice Hall, Upper Saddle River (1987)
15. Wang, J.T., Zhang, C.H., Du, X.L.: An explicit integration scheme for solving dynamic problems of solid and porous media. J. Earthq. Eng. **12**(2), 293–311 (2008)
16. Rezaiee, Pajand M., Sarafrazi, S.R., Hashemian, M.: Improving stability domains of the implicit higher order accuracy method. Int. J. Numer. Methods Eng. **88**(9), 880–896 (2011)

17. Franklin, G.F., Powell, J.D., Emami Naeini, A.: Feedback Control of Dynamic Systems. Prentice Hall, Upper Saddle River (2002)
18. Ramirez, M.R.: The numerical transfer function for time integration analysis. Proceedings of New Methods in Transient Analysis, ASME, New York, PVP, vol. 246, pp. 79–85 (1992)
19. Mugan, A., Hulbert, G.: Frequency-domain analysis of time-integration methods for semidiscrete finite element equations, part I: parabolic problems. Int. J. Numer. Methods Eng. **51**(3), 333–350 (2001)
20. Mugan, A., Hulbert, G.M.: Frequency-domain analysis of time-integration methods for semidiscrete finite element equations, part II: hyperbolic and parabolic–hyperbolic problems. Int. J. Numer. Methods Eng. **51**(3), 351–376 (2001)
21. Chen, C., Ricles, J.M.: Stability analysis of direct integration algorithms applied to nonlinear structural dynamics. J. Eng. Mech. ASCE **134**, 703 (2008)
22. Chen, C., Ricles, J.M.: Stability analysis of direct integration algorithms applied to MDOF nonlinear structural dynamics. J. Eng. Mech. ASCE **136**, 485 (2010)
23. Ogata, K.: Discrete-Time Control Systems. Prentice Hall, Upper Saddle River (1995)
24. Chopra, A.K., Naeim, F.: Dynamics of Structures: Theory and Applications to Earthquake Engineering. Prentice Hall, Upper Saddle River (2007)
25. Bathe, K.J., Wilson, E.L.: Numerical Methods in Finite Element Analysis. Prentice Hall, Upper Saddle River (1976)
26. MathWorks, Inc.: Matlab, 2006b. MathWorks, Inc., Natick, MA (2006)
27. Wereley, N.M., Pang, L., Kamath, G.M.: Idealized hysteresis modeling of electrorheological and magnetorheological dampers. J. Intell. Mater. Syst. Struct. **9**(8), 642–649 (1998)